UDC 621.701.12
https://doi.org/10.17073/0021-3438-2025-4-50-61

Research article
Научная статья

Influence of plasma narrow-jet cutting parameters on the weld quality during laser welding of titanium alloys

S.V. Anakhov[1], **B.N. Guzanov**[1], **N.S. Michurov**[2]

[1] **Russian State Vocational Pedagogical University**
11 Mashinostroiteley Str., Ekaterinburg 620012, Russia

[2] **Ural Institute of State Fire Service of EMERCOM**
22 Mira Str., Ekaterinburg 620062, Russia

✉ Sergey V. Anakhov (sergej.anahov@rsvpu.ru)

Abstract: The study investigates the structural and mechanical characteristics of permanent joints produced by laser welding of VT1-0/VT1-0 titanium alloys after cutting with a newly designed PMVR-5.3 narrow-jet plasma torch, which features a gas-dynamic stabilization (GDS) system with several design innovations. The improved GDS efficiency enhances cutting precision and surface quality, thereby increasing the radiation absorption coefficient, weld penetration, and overall laser-welding efficiency. Experimental results show that continuous-wave CO_2 laser welding of VT1-0/VT1-0 plates forms a narrow weld with a structure corresponding to the as-cast state of the alloy and large equiaxed grains in the central part of the weld, which decrease in size toward the root compared with those in the surface region. Although gas shielding does not completely prevent the formation of fine micropores in the weld metal, their amount is insignificant; they do not form critical clusters within the microvolumes of the weld and have no adverse effect on the strength characteristics of the welded joint. The average microhardness of the weld metal was found to be higher than that of the base metal. According to tensile and microhardness testing, the weld metal demonstrates high strength, significantly exceeding that of the titanium alloy, and exhibits a ductile fracture morphology. Under cyclic loading, fracture occurred in the base metal rather than in the weld metal, with the fraction of the final rupture zones increasing as the maximum cyclic stress rose. The findings confirm the applicability of precision narrow-jet air-plasma cutting and continuous-wave CO_2 laser welding technologies for producing VT1-0/VT1-0 welded joints with high efficiency and mechanical strength comparable to those of the base material.

Keywords: laser welding, plasma cutting, titanium alloys, weld metal, heat-affected zone, structural transformations, defects, quality, efficiency.

Acknowledgements: The work was supported by the Russian Science Foundation, grant No. 23-29-00111.

The authors thank E.B. Trushina for assistance with fractographic examination of specimen fracture surfaces after mechanical testing, and D.I. Vychuzhanin (Cand. Sci. (Eng.)), for assistance with the mechanical tests.

For citation: Anakhov S.V., Guzanov B.N., Michurov N.S. Influence of plasma narrow-jet cutting parameters on the weld quality during laser welding of titanium alloys. *Izvestiya. Non-Ferrous Metallurgy.* 2025;31(4):50–61. https://doi.org/10.17073/0021-3438-2025-4-50-61

© 2025 S.V. Anakhov, B.N. Guzanov, N.S. Michurov

Влияние особенностей плазменной узкоструйной резки на качество сварного шва при лазерной сварке титановых сплавов

С.В. Анахов[1], **Б.Н. Гузанов**[1], **Н.С. Мичуров**[2]

[1] **Российский государственный профессионально-педагогический университет**
Россия, 620012, г. Екатеринбург, ул. Машиностроителей, 11

[2] **Уральский институт государственной противопожарной службы МЧС России**
Россия, 620062, Екатеринбург, ул. Мира, 22

✉ Сергей Вадимович Анахов (sergej.anahov@rsvpu.ru)

Аннотация: Исследованы особенности формирования структуры и свойств неразъемных соединений при лазерной сварке титановых сплавов типа ВТ1-0/ВТ1-0, полученных после резки новым узкоструйным плазмотроном типа ПМВР-5.3, имеющим ряд конструктивных особенностей в системе газодинамической стабилизации (ГДС) плазменной дуги. Достигнутое преимущество в эффективности ГДС способствует повышению степени прецизионности и качества реза и, как следствие, увеличению коэффициента поглощения излучения, коэффициента проплавления и эффективности лазерной сварки. По результатам исследований показано, что при получении углекислотным лазером сварных соединений типа ВТ1-0/ВТ1-0 происходит формирование узкого шва со структурой, соответствующей литому состоянию сплава, и участков с крупными равноосными зернами в центральной части шва, уменьшающимися по размерам в донной части по сравнению с расположенными в поверхностной области. Защита сплава от газонасыщения в структуре сварного шва не позволяет избежать формирования мелких микропор в структуре сварного шва, однако их количество незначительно и они не создают критических скоплений в микрообъемах шва и не влияют на прочностные характеристики неразъемного соединения, при этом средние значения микротвердости материала шва выше, чем материала основы. В результате испытаний на статическое растяжение, а также определения значения микротвердости установлено, что материал сварного шва является достаточно прочным и существенно превышает прочность самого титанового сплава, а рельеф поверхности разрушения образцов соответствует вязкому разрушению. При циклических испытаниях образцов сварных соединений разрушение происходило не по шву, а по основному металлу с ростом доли зон долома в сечении образцов при увеличении значений максимального напряжения цикла. По результатам исследований можно сделать вывод о применимости технологий прецизионной узкоструйной воздушно-плазменной резки и сварки углекислотным лазером непрерывного действия для реализации процесса получения сварных соединений ВТ1-0/ВТ1-0 с высокой степенью эффективности и прочности на уровне соединяемых материалов.

Ключевые слова: лазерная сварка, плазменная резка, титановые сплавы, сварной шов, зона термического влияния, структурные превращения, дефекты, качество, эффективность.

Благодарности: Работа выполнена при поддержке гранта РНФ № 23-29-00111.

Авторы выражают благодарность Е.Б. Трушиной за помощь в проведении исследований фрактографии поверхности образцов после механического испытания и к.т.н. Д.И. Вычужанину за помощь в проведении механических испытаний.

Для цитирования: Анахов С.В., Гузанов Б.Н., Мичуров Н.С. Влияние особенностей плазменной узкоструйной резки на качество сварного шва при лазерной сварке титановых сплавов. *Известия вузов. Цветная металлургия*. 2025;31(4):50–61.
https://doi.org/10.17073/0021-3438-2025-4-50-61

Introduction

Extensive research on titanium and its alloys conducted in recent years has unequivocally demonstrated that, in terms of their physical, mechanical, chemical, and technological properties, these materials surpass most modern structural alloys, including the most common ones such as steel and aluminum. The continuous growth in their application is attributed to the fact that titanium alloys combine low density with high strength and heat resistance at moderate temperatures while maintaining excellent corrosion resistance. These ad-

vantages have made titanium a versatile structural material, particularly in high-technology industries where titanium alloys with diverse properties are often essential — or even irreplaceable — for strategic sectors such as aerospace, nuclear power, shipbuilding, and chemical engineering [1—3].

The development of welding methods capable of producing high-quality, permanent joints has significantly expanded the use of titanium and its alloys in manufacturing complex engineering components and metal structures. However, welding titanium alloys presents certain technological challenges. These are primarily associated with the high chemical reactivity of titanium with nitrogen, oxygen, and hydrogen at elevated temperatures and in the molten state. As a result, the material may lose ductility due to the formation of stable compounds with atmospheric gases, as well as develop defects such as porosity. To prevent such issues, it is essential to ensure reliable shielding of both the weld zone and the root side from atmospheric contamination and to minimize the heating time of the joint during welding [4].

A major drawback of titanium alloys is their tendency to form a coarse-grained structure during welding, both in the weld metal and in the heat-affected zone (HAZ). This structural heterogeneity leads to a decrease in the mechanical strength of the joint due to the formation of a microstructure that differs from that of the base metal [5; 6]. Since different regions within the welded joint are exposed to varying thermal cycles, grains of different sizes form, complicating the selection of welding parameters that minimize the thermal impact on the HAZ. From this perspective, laser welding is considered a promising alternative to conventional welding methods [7]. The localized and short-duration high-energy exposure of the laser beam provides the most favorable conditions for forming sound welds in titanium and its alloys [8; 9].

Technologies and research objective

While laser technologies have a number of undeniable advantages in welding processes for the fabrication of various metal structures [10; 11], certain features of beam processing must also be taken into account. Chief among them is the relatively low efficiency of the process, as the effectiveness of laser welding largely depends on the reflective properties of the metal surface. Several approaches are known to improve the absorption coefficient — and consequently, the penetration depth and overall welding efficiency. As demonstrated in [12], the absorption coefficient is affected by the material properties, as well as by the quality and method of edge preparation, which determine surface roughness and the geometry of the joint gap in butt-welded plates. Comprehensive studies evaluating the relationship between absorption coefficient and cut-edge quality have shown a significant increase in reflected radiation from rougher surfaces compared with polished ones [13—15]. Thus, it should be noted that surface roughness produced during sheet cutting in the preparation stage varies widely depending on the cutting method used.

The authors conducted comparative studies to evaluate the cut-edge quality achieved using various high-energy cutting techniques for the preparation of welded joints. The results indicated that the most favorable outcomes across all standardized parameters were obtained when using precision air—plasma cutting of metallic materials with the PMVR-5.3 plasma torch, developed by NPO Polygon LLC (Ekaterinburg, Russia) [16]. A distinctive feature of this design is the implementation of a new gas—air flow path with symmetric plasma-forming gas injection into the flow-splitting system and a gas-dynamic flow stabilizer. The stabilizer employs two swirlers (forming and stabilizing) with a variable number of swirl channels, providing efficient gas-vortex stabilization of the plasma arc. The evaluation focused on standardized quality indicators such as the presence of burrs, droplets, and temper colors, as well as oscillations (variations in the linearity of surface micro-irregularities) and deviation of the cut edge from verticality. To substantiate the visual inspection results quantitatively, surface microrelief parameters were measured using a TR-200 surface roughness tester [17]. The results are presented in Table 1.

According to geometric and surface-quality characteristics after high-energy cutting, the most favorable results for subsequent laser welding were obtained using the PMVR-5.3 plasma torch, designed as a domestic alternative to imported plasma systems of this class. Moreover, as demonstrated in [17], enhanced weld penetration and improved weld formation during laser processing were achieved when the cut-edge roughness ranged between $Ra \approx 2.0 \div 6.3$ μm, which promotes a higher absorption coefficient on the prepared surfaces. With further increases in roughness, however, the joint gap between the welded plates widens, allowing a substantial portion of the laser beam to pass through without absorption. Consequently, the absorption coefficient decreases, resulting in lower weld quality and a higher incidence of defects.

Table 1. **Comparison of average surface roughness parameters for various high-temperature cutting technologies**

Таблица 1. Сравнение средних показателей шероховатости реза при различных технологиях высокотемпературной разделки

Specimen	Cutting technology	Equipment	Cutting parameters	*Ra*	*Rz*	*Rt*
1	Air–plasma	Plasma torch YK200H (Huayuan FLG-400HD, China)	I = 175 A U = 155 B V = 1500 mm/min D_{nozzle} = 1.9 mm	3.30	4.22	34.82
2	Air–plasma	Plasma torch PMVR-5.3 (NPO Polygon LLC, Russia)	I = 175 A U = 137 B V = 1500 mm/min D_{nozzle} = 1.9 mm P = 4.5 atm	2.17	2.70	58.48
3	Gas–oxygen	Mechanized gas-cutting system Longteng (China)	P_{O_2} = 5 atm $P_{C_3H_8}$ = 0.5 atm V = 1500 mm/min	3.71	4.65	33.86
4	Laser	Trulaser 5030 Classic, CO_2 (Trumpf Group, Germany)	N = 1,7 kW f = 2 kHz V = 600 mm/min P = 0.6 bar	10.78	12.61	69.41

In view of the above, the objective of this study was to investigate the structural and mechanical characteristics of permanent joints formed during laser welding of titanium alloys, where the plates were cut using narrow-jet air—plasma cutting technology implemented with the PMVR-5.3 plasma torch.

Materials and methods

Titanium alloys are known for their tendency to undergo hardening due to the presence of alloying elements that promote the formation of nonequilibrium microstructures and reduce ductility, sometimes resulting in cold cracking [18, 19]. For this reason, commercially pure titanium VT1-0 was selected as the material for this study. During welding, this alloy forms a cast structure characteristic of pure titanium in the joint zone, allowing the assessment of weld quality without the influence of additional phase or structural transformations.

Laser welding of 3 mm-thick titanium plates, previously cut by plasma, was carried out using a continuous-wave CO_2 laser with a maximum power of 3 kW. The laser was equipped with a zinc selenide (ZnSe) focusing lens (focal length 254 mm) and produced a plane-polarized beam with a diameter of 30 mm. The welding parameters were as follows: welding speed V = = 46.6 mm/s, laser power W = 2.1 kW, and focal offset F = 0 mm. Protection of the weld pool and heat-affected zone was provided by a shielding gas mixture of carbon dioxide and air in a ratio of 1 : 7, in accordance with GOST R ISO 14175-2010[1], at a pressure of 12 Torr (1.6 kPa). Metallographic analysis was performed using an optical microscope Neophot 21 (Germany). The titanium structure and weld morphology were revealed by chemical etching, which was also used to prepare the surface for microindentation testing. The weld and adjacent zones were analyzed on specimens cut from different areas of the joint, taking into account structural features formed during solidification following high-temperature processing. Grain size was determined in accordance with GOST 21073.3-75[2]

[1] GOST R ISO 14175-2010. Welding materials. Gases and gas mixtures for fusion welding and related processes. Moscow: Standartinform, 2011. (In Russ.).

[2] GOST 21073.3-75. Non-ferrous metals. Determination of grain size by counting border crossings. Moscow: Publ. Standards, 2002. (In Russ.).

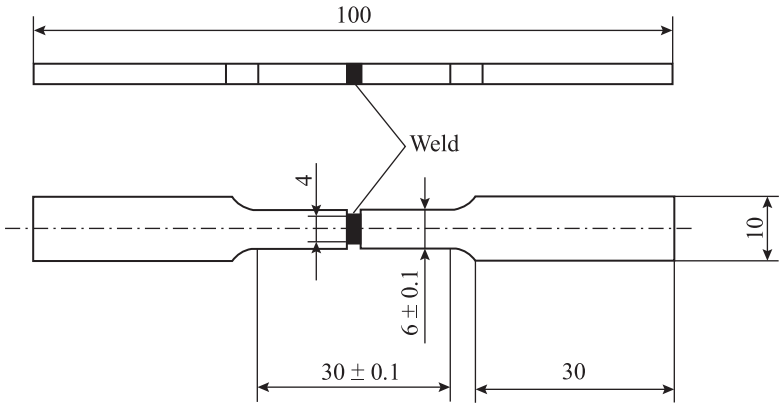

Fig. 1. Schematic representation of the specimen used for tensile testing

Рис. 1. Схематическое изображение образца для испытаний на растяжение

using the grain boundary intersection counting method. Microhardness across the weld was measured by instrumented Vickers microindentation using a Fischerscope HM 2000 XYm microhardness tester (Helmut Fischer GmbH, Germany). The tensile strength of the welded joints was evaluated using a servo-hydraulic testing machine Instron 8801 (Instron, USA) in accordance with GOST 6996-66[1]. Flat specimens of type B, designed for determining weld metal strength, were used. To ensure fracture propagation through the weld, a special notch was machined along the weld width, reducing the cross-sectional area of the specimen by 30 % (see Fig. 1).

Cyclic fatigue tests on flat specimens were performed under a sinusoidal loading cycle at a frequency of 5 Hz and a stress ratio (R) = 0, in accordance with RD 50-345-82[2]. The fracture surface morphology after mechanical testing was examined using a Tescan Vega-II XMU scanning electron microscope (Carl Zeiss, Czech Republic) and described following the terminology and definitions specified in RD 50-672-88[3].

Results and discussion

During the formation of the VT1-0/VT1-0 welded joint, a narrow weld was obtained with a shape factor (the ratio of penetration depth to weld width) of 2.5 (Fig. 2). Despite the high cooling rates, the grain size in both the fusion zone (FZ) and the heat-affected zone (HAZ) was significantly larger than in the base metal (Table 2). The structure of the FZ corresponds to the as-cast state of titanium: the central region consists of equiaxed polyhedral grains, while the outer regions are composed of larger, elongated grains oriented along the direction of heat removal (Fig. 3, *a*). In the lower portion of the weld, the grains were 1.5—2 times smaller and more equiaxed compared to those in the upper surface area (Fig. 3, *b*).

The microstructure of the as-cast VT1-0 alloy consists of β-transformed grains of about 300 μm, containing parallel α-lamellae 4—10 μm thick, with a length comparable to the size of the prior β-grains. It is known [20; 21], that during the β → α polymorphic transformation, the α-phase grows according to the principle of orientation and dimensional conformity, forming parallel α-lamellae aligned in the same direction. As a result, colonies of α-lamellae form a characteristic intragranular texture within the former β-grains.

At the interface between the heat-affected zone (HAZ) and the base metal, a mixed microstructure was formed, consisting of light-colored polyhedral β-phase grains and α-phase lamellae (Fig. 3, *c*). It should be noted that the α-phase grain size in the HAZ was approximately 1.5—2 times larger than in the base metal (Table 2). Overall, the HAZ material was characterized as partially recrystallized, containing numerous deformed α-phase grains with a high level of residual stresses, which affect crystal orienta-

[1] GOST 6996-66. Welded joints. Methods for determining mechanical properties. Moscow: Standartinform, 2006. (In Russ.).

[2] RD 50-345-82. Methodological guidelines. Calculations and strength tests in mechanical engineering. Methods of cyclic testing of metals. Determination of crack resistance characteristics (fracture toughness) under cyclic loading. Moscow: Publ. Standards, 1983. (In Russ.).

[3] RD 50-672-88. Methodological guidelines. Calculations and strength tests. Classification of types of metal fractures. Moscow: Publ. Standards, 1989. (In Russ.).

Table 2. **Characteristics of the VT1-0/VT1-0 welded joint material**

Таблица 2. Характеристики материала сварного соединения ВТ1-0/ВТ1-0

Specimen	FZ parameters				HAZ parameters				Grain size, μm		
	l, mm	$HV_{0.05}$			*l*, mm	$HV_{0.05}$			Base metal	HAZ	FZ
		max	min	average		max	min	average			
1	1,2	370	210	280	0,75	280	195	230	20	40	300
2	1,2	275	175	230	0,70	275	220	247	20	50	300

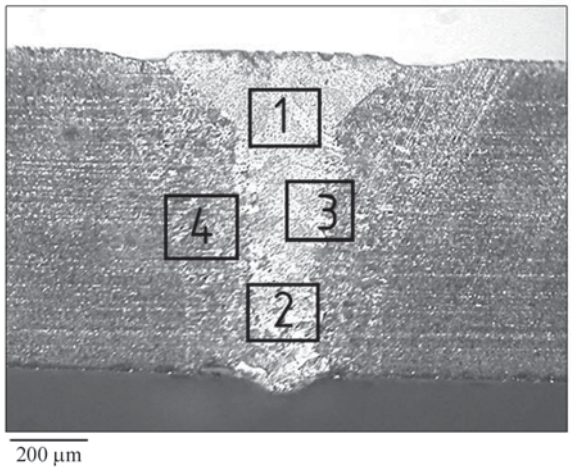

Fig. 2. Macrostructure of the VT1-0/VT1-0 welded joint

Рис. 2. Макроструктура сварного соединения ВТ1-0/ВТ1-0

tion, promote texture formation, and determine the specific features of the structure formation in the weld metal itself (Fig. 3, *d*).

The examination showed that, despite shielding protection against gas absorption, the weld structure contained small micropores about 2—3 μm in size, which can be observed in the micrograph of a local area of the chevron fracture (Fig. 7, *b*). It should be noted that their number is insignificant, and they do not form critical clusters within the microvolumes of the weld metal and, overall, have no effect on the strength characteristics of the welded joint (Table 3). VT1-0, being a single-phase α-alloy, contains a small amount of secondary β-phase, which appears as thin lamellae along the α-grain boundaries. The two-phase structure causes a nonuniform microhardness distribution, where minimum values correspond to the β-phase and maximum to the α-phase [22]. As shown above, the weld metal exhibits a mixed microstructure in which β-phase—enriched regions, upon rapid solidification from the melt, attain high strength. This leads to an overall increase in the average microhardness across the weld width, reaching its maximum in the cast microstructure of the weld metal [23]. At the same time, the refinement of the formed phases contributed to a greater scatter of microhardness values along the measurement line. The averaged microhardness distribution is presented in Fig. 4.

Tensile test results showed that, despite minor internal porosity, the weld metal exhibited high strength (Table 3), significantly exceeding that of the base alloy. The fracture surface morphology after static tension corresponded to ductile failure (Fig. 5, *a*, *b*). The fracture surface of the weld metal contained dimples of varying depth and isolated regions of cellular relief—clusters of small, flat dimples resembling a honeycomb pattern (Fig. 5, *b*), typical for the fracture of cast alloys. This morphology indicates a limited degree of local plastic deformation at failure, but still belongs to the ductile fracture mode, characteristic of plastic materials [20; 24].

During cyclic testing of VT1-0/VT1-0 welded joint specimens at a stress ratio of $\sigma/\sigma_в \geq 0.72$, fracture occurred not along the weld metal but within the base metal. In this case, considerable plastic deformation was observed, accompanied by the formation of a neck during the final loading cycles. This phenomenon is explained by the fact that the VT1-0 alloy exhibits cyclic softening behavior [18].

The fracture surfaces of all specimens displayed characteristic features of fatigue fracture — distinct surface regions differing in morphology, including the crack initiation area, fatigue striations, and ridges representing traces of coalescence of separately initiated neighboring cracks propagating in the same direction, usually from the initiation site. In addition, final fracture zones with features of ductile failure were identified. The fracture surface morphology of VT1-0/VT1-0 welded joint specimens is shown in Fig. 6.

Table 3. **Mechanical test results for VT1-0/VT1-0 welded joint specimens**

Таблица 3. Результаты механических испытаний образцов сварного соединения ВТ1-0/ВТ1-0

Specimen	Material	Tensile test		Fatigue test		
		Fracture location	σ_u, MPa	Number of cycles	σ, MPa	σ/σ_u*
1	Base metal	–	500	Not determined		
2	Weld metal	Weld metal	620	5770	433	0.7
3	Weld metal	Weld metal	660	485856	257	0.4

* Specimens were compared at equal ratios of the maximum cyclic stress (σ) to the ultimate tensile strength (σ_u) determined in tensile tests.

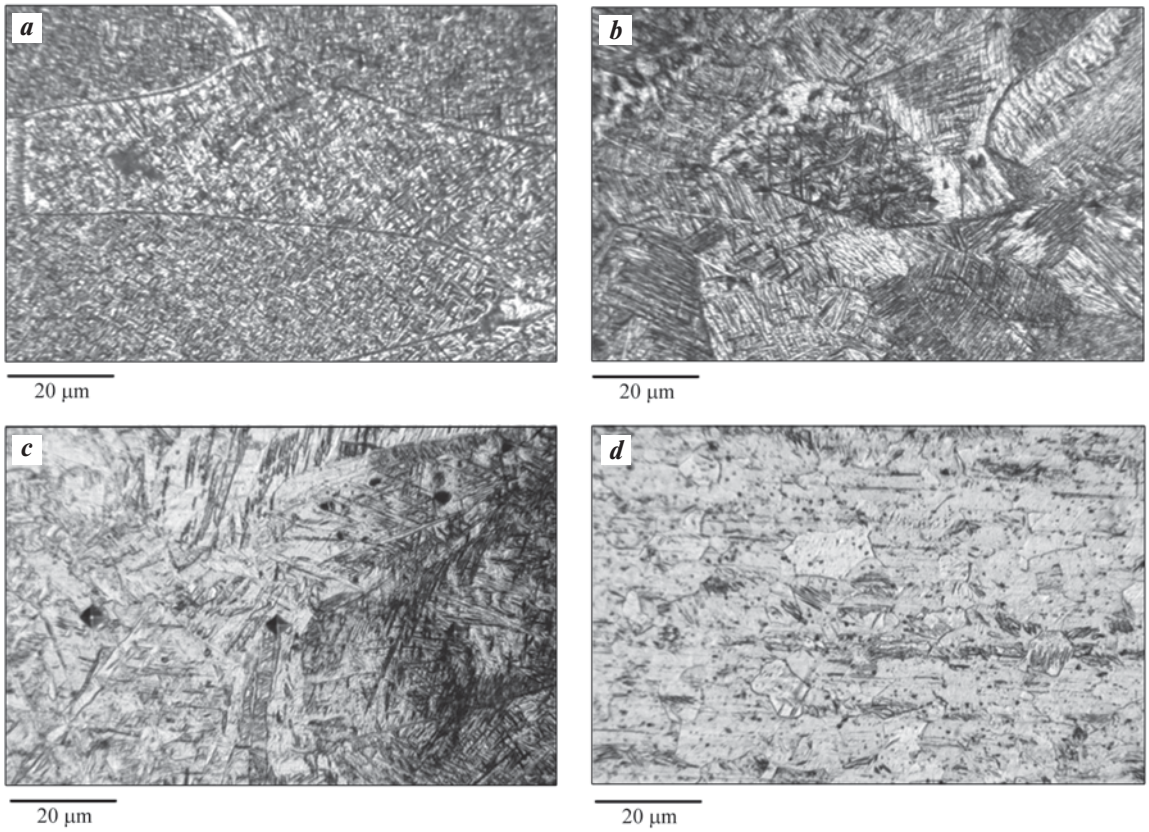

Fig. 3. Microstructure of the VT1-0/VT1-0 welded joint

a – upper part of the fusion zone (area *1* in Fig. 2); ***b*** – root of the fusion zone (area *2* in Fig. 2); ***c*** – boundary between FZ and HAZ (area *3* in Fig. 2); ***d*** – heat-affected zone (area *4* in Fig. 2)

Рис. 3. Микроструктура сварного соединения ВТ1-0/ВТ1-0

a – верхняя часть ЗСШ (зона *1* на рис. 2); ***b*** – корень ЗСШ (зона *2* на рис. 2); ***c*** – граница ЗСШ и ЗТВ (зона *3* на рис. 2); ***d*** – ЗТВ (зона *4* на рис. 2)

Fracture in the crack-initiation regions is brittle and feather-like, propagating along several directions. While the overall direction of fatigue crack growth is preserved, it changes in neighboring grains (Fig. 7, *a*). This behavior is governed by the lamellar α-phase morphology in the weld metal: smooth, polished facets alternate with relief steps that might be mistaken for cleavage, although they are, in fact, the lateral surfaces of α-lamellae.

In the vicinity of micropores, local areas of chevron fracture were observed (arrowed in Fig. 7, *b*). This fea-

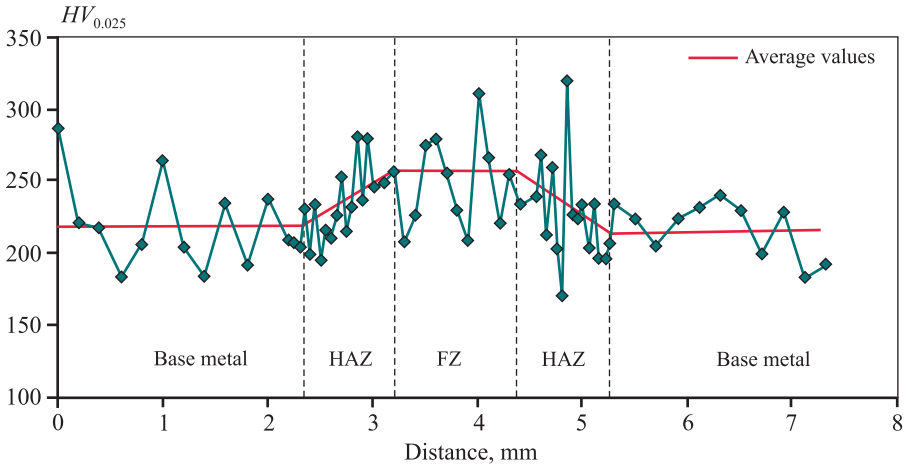

Fig. 4. Variation of microhardness across the width of the VT1-0/VT1-0 welded joint

Рис. 4. Характер изменения микротвердости по ширине сварного соединения ВТ1-0/ВТ1-0

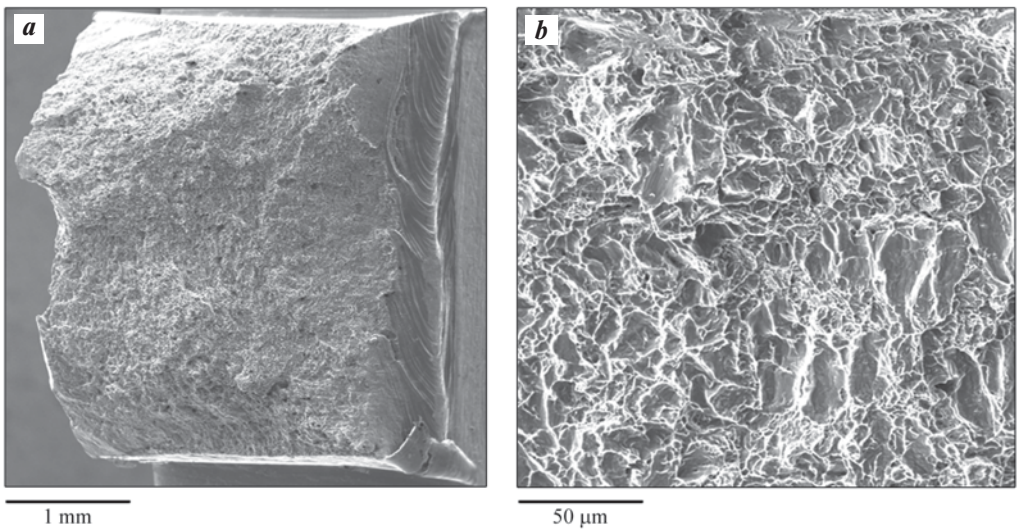

Fig. 5. Macro- (***a***) and micro- (***b***) relief of the fracture surfaces of a VT1-0/VT1-0 welded joint specimen after tensile testing

Рис. 5. Макро- (***a***) и микро- (***b***) рельеф поверхности разрушения образца сварного соединения ВТ1-0/ВТ1-0 после статического растяжения

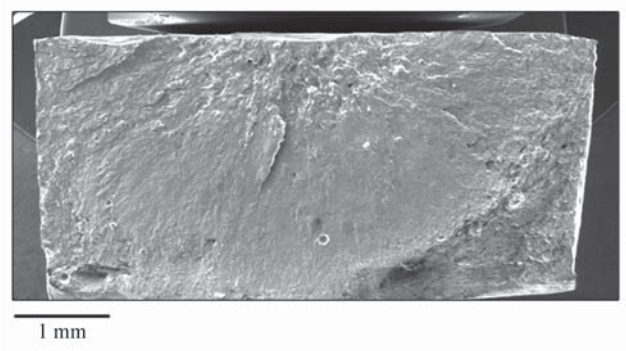

Fig. 6. Macroscopic fracture surface of a VT1-0/VT1-0 welded joint specimen at a maximum cyclic load of 265 MPa

Рис. 6. Макрорельеф поверхности разрушения образца сварного соединения ВТ1-0/ВТ1-0 при максимальной нагрузке цикла 265 МПа

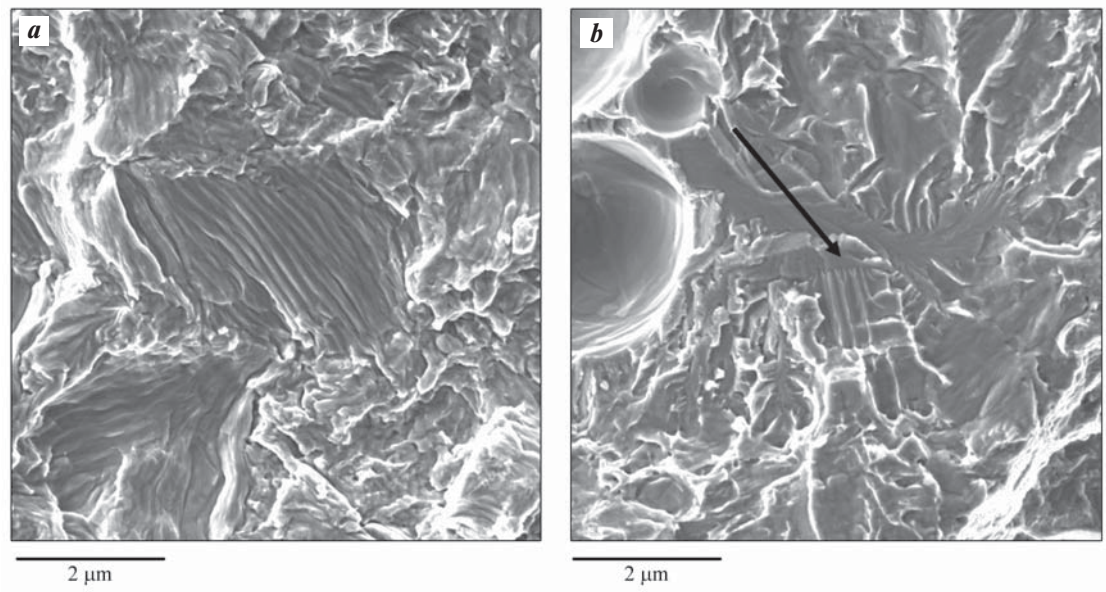

Fig. 7. Macroscopic fracture surface of a VT1-0 alloy specimen
a – change in fatigue crack propagation direction near the initiation site
b – microregion of a chevron fracture near a micropore (indicated by an arrow)

Рис. 7. Микрорельеф поверхности разрушения образца сплава ВТ1-0
a – изменение направления роста усталостной трещины вблизи очага
b – микроучасток шевронного излома вблизи микропоры (отмечен стрелкой)

ture indicates limited plastic deformation and forms under tension with bending in regions of unstable crack growth or during brittle transgranular fatigue fracture. The pores deflect the path of fatigue cracks, which appears as changes in the orientation of fatigue striations. Within initiation zones, isolated areas of ductile fatigue fracture with striations and plateaus, as well as segments of intergranular fatigue crack growth, are present.

Analysis of fracture-surface relief after fatigue tests at different maximum cyclic stresses showed that, at a maximum cyclic stress of 264 MPa, the final rupture zone occupied 35 vol. % of the specimen cross-section. Under these conditions, the area ratio of the fatigue-fracture zone to the final-rupture zone increased to 1.9. In all examined specimens, the final rupture zones exhibited a dimpled fracture with relatively deep dimples, indicating high fracture energy.

As the maximum cyclic stress increased, the fraction of the final rupture zone in the cross-section increased as expected; at a maximum cyclic stress of 425 MPa, these zones occupied 55 vol. %. This finding indicates a substantial contribution of the final rupture zone to the strength of titanium alloy specimens with welded joints under fatigue loading. Since a dimpled fracture corresponds to relatively high fracture energy, the specimens that endured a greater number of cycles were those in which the volume of material involved in fatigue crack growth was about half that of the final rupture zone.

Conclusions

1. Precision narrow-jet air—plasma cutting with PMVR-5.3 torches is suitable for joint preparation, delivering high cut accuracy and surface quality while increasing the absorption coefficient — and, consequently, weld penetration and overall laser-welding efficiency.

2. Continuous-wave CO_2 laser welding of VT1-0/VT1-0 produces a narrow weld whose structure corresponds to the as-cast state of the alloy. The central weld region contains large equiaxed grains that become elongated along the heat-flow direction toward the boundaries and decrease in size toward the root compared with the surface region. The weld microstructure comprises light polyhedral grains and α-phase lamellae; in the HAZ, the α-phase grain size is 1.5—2.0 times larger than in the base metal.

3. Shielding does not completely eliminate fine micropores in the weld metal, which leads to a nonuniform microhardness distribution. Nevertheless, owing to the fine-lamellar α-phase morphology, the average

microhardness in the weld metal is somewhat higher than in the base metal. Tensile tests show that, despite minor porosity, the weld metal exhibits high strength, significantly exceeding that of the base alloy, and the fracture surface morphology corresponds to ductile failure.

4. Under cyclic loading, VT1-0/VT1-0 specimens fracture in the base metal rather than in the weld metal. With increasing maximum cyclic stress, the fraction of the final rupture zone increases, indicating its substantial contribution to the strength of welded titanium alloy specimens under fatigue loading.

5. The combined use of precision narrow-jet air—plasma cutting and continuous-wave CO_2 laser welding enables the fabrication of VT1-0/VT1-0 welded joints with high efficiency and strength comparable to the parent material.

References

1. Aleksandrov A.V., Lednov S.V., Davydkina E.A. State of the affairs in the titanium industry and development prospects. *Tekhnologiya legkikh splavov*. 2021;(2):76—81. (In Russ.).
https://doi.org/10.24412/0321-4664-2021-2-76-81
Александров А.В., Леднов С.В., Давыдкина Е.А. Состояние дел в титановой отрасли и перспективы развития. *Технология легких сплавов*. 2021;(2):76—81. https://doi.org/10.24412/0321-4664-2021-2-76-81
2. Kishawy H.A., Hosseini A. Machining difficult-to-cut materials. Chapter: Titanium and titanium alloys. Springer: Ser. Materials forming, machining and tribology, 2019.
https://doi.org/10.1007/978-3-319-95966-5_3
3. Bubnov V.A., Knyazev A.N. Titanium and its alloys in mechanical engineering. *Bulletin of Kurgan State University*. 2016;(3):92—96. (In Russ.).
Бубнов В.А., Князев А.Н. Титан и его сплавы в машиностроении. *Вестник Курганского государственного университета*. 2016;(3):92—96.
4. Pultsin N.M. Interaction of titanium with gases. Moscow: Metallurgiya, 1969. 213 p. (In Russ.).
Пульцин Н.М. Взаимодействие титана с газами. М.: Металлургия, 1969. 213 с.
5. Ilyin A.A. Mechanism and kinetics of phase and structural transformations in titanium alloys. Moscow: Nauka, 1994. 304 p. (In Russ.).
Ильин А.А. Механизм и кинетика фазовых и структурных превращений в титановых сплавах. М.: Наука, 1994. 304 с.
6. Germain L., Gey N., Humbert M., Vo P., Jahazi M., Bocher Ph. Texture heterogeneities induced by subtransus processing of near α titanium alloys. *Acta Materialia*. 2008;56(15):4298—4308.
7. Groche P., Wohletz S., Brenneis M., Pabst P., Resch F. Joining by forming — A review on joint mechanisms, applications and future trends. *Journal of Materials Processing Technology*. 2014;212(10):1972—1994.
8. Paton B.E., Shelyagin V.D., Akhonin S.V., Topolskii V.F., Khaskin V.Yu., Petrichenko I.K., Bernatskii A.V., Mishchenko R.N., Siora A.V. Laser welding of titanium alloys. *Avtomaticheskaya svarka*. 2009;(10):35—39. (In Russ.).
Патон Б.Е., Шелягин В.Д., Ахонин С.В., Тополь-ский В.Ф., Хаскин В.Ю., Петриченко И.К., Бернацкий А.В., Мищенко Р.Н., Сиора А.В. Лазерная сварка титановых сплавов. *Автоматическая сварка*. 2009;(10):35—39.
9. Sokolov M., Salminen A. Improving laser beam welding efficiency. *Engineering*. 2014;6(09):559—571.
https://doi.org/10.4236/ENG.2014.69057
10. Akman E., Demir A., Canel T., Sınmazçelik T. Laser welding of Ti6Al4V titanium alloys. *Journal of Materials Processing Technology*. 2009;209(8):3705—3713.
https://doi.org/10.1016/j.jmatprotec.2008.08.026
11. Zhang Y., Sun D., Gu X., Li H. A hybrid joint based on two kinds of bonding mechanisms for titanium. *Materials Letters*. 2016;15(185):152—155.
12. Riccardi G., Cantello M. Laser material interactions: Absorption coefficient in welding and surface treatment. *CIRP Annals — Manufacturing Technology*. 1994;1:171—175.
https://doi.org/10.1016/j.optlastec.2012.03.025
13. Sokolov M., Salminen A. Experimental investigation of the influence of edge morphology in high power fiber laser welding. *Physics Procedia*. 2012;39:33—42.
https://doi.org/10.1016/j.phpro.2012.10.0115
14. Covelli L., Jovane F., De Lori L., Tagliaferri V. Laser welding of stainless steel: Influence of the edges morphology. *CIRP Annals — Manufacturing Technology*. 1988;37:545—548.
15. Sokolov M., Salminen A., Somonov V., Kaplan A.F. Laser welding of structural steels: Influence of the edge roughness level. *Optics & Laser Technology*. 2012;44(7):2064—2071.
16. Pykin Yu.A., Anakhov S.V., Matushkin A.V. Plasmatron: Patent 2754817 (RF). 2021. (In Russ.).
Пыкин Ю.А., Анахов С.В., Матушкин А.В. Плазмотрон: Патент 2754817 (РФ). 2021.

17. Anakhov S.V., Guzanov B.N., Matushkin A.V., Michurov N.S. On compliance with regulatory standards for cutting quality in the production of welded joints. *Competency*. 2024;(5):56—62. (In Russ.).
https://doi.org/10.24412/1993-8780-2024-5-56-62
Анахов С.В., Гузанов Б.Н., Матушкин А.В., Мичуров Н.С. О соблюдении регламентных норм на качество резки при производстве сварных соединений. *Компетентность*. 2024;(5):56—62.
https://doi.org/10.24412/1993-8780-2024-5-56-62
18. Ilyin A.A., Kolachev B.A., Polkin I.S. Titanium alloys. Composition, structure, properties. Moscow: VILS–MATI, 2009. 520 p. (In Russ.).
Ильин А.А., Колачев Б.А., Полькин И.С. Титановые сплавы. Состав, структура, свойства: Справочник. М.: ВИЛС—МАТИ, 2009. 520 с.
19. Illarionov A.G., Popov A.A. Technological and operational properties of titanium alloys. Ekaterinburg: Ural University Press, 2014. 137 p. (In Russ.).
Илларионов А.Г., Попов А.А. Технологические и эксплуатационные свойства титановых сплавов. Екатеринбург: Изд-во Уральского университета, 2014. 137 с.
20. Klevtsov G.V., Botvina L.R., Klevtsova N.A., Limar L.V. Fractodiagnostics of destruction of metal materials and structures. Moscow: MISIS, 2007. 264 p. (In Russ.).
Клевцов Г.В., Ботвина Л.Р., Клевцова Н.А., Лимарь Л.В. Фрактодиагностика разрушения металлических материалов и конструкций. Учеб. пос. для вузов. М.: МИСИС, 2007. 264 с.
21. Gnusov S.F., Klimenov V.A., Alkhimov Yu.V., Budnitsky A.D., Orishich A.M., Cherepanov A.N., Afonin Yu.V. Formation of the structure of titanium and corrosion-resistant steel during laser welding. *Welding International*. 2012;(1):17—22.
22. Ivanov M.B., Kolobov Yu.R., Manokhin S.S., Golosov E.V. Investigation of the structural and phase state of medical titanium alloys by modern methods of analytical electron microscopy. *Indusrial laboratory. Diagnostics of materials*. 2012;78(1):43—54. (In Russ.).
Иванов М.Б., Колобов Ю.Р., Манохин С.С., Голосов Е.В. Исследование структурно-фазового состояния медицинских титановых сплавов современными методами аналитической электронной микроскопии. *Заводская лаборатория. Диагностика материалов*. 2012;78(1):43—54.
23. Polkin I.S., Egorova Yu.B., Davydenko L.V. Alloying, phase composition and mechanical properties of titanium alloys. *Tekhnologiya legkikh splavov*. 2022;(2): 4—13. (In Russ.).
https://doi.org/10.24412/0321-4664-2022-2-4-13
Полькин И.С., Егорова Ю.Б., Давыденко Л.В. Легирование, фазовый состав и механические свойства титановых сплавов. *Технология легких сплавов*. 2022;(2):4—13.
https://doi.org/10.24412/0321-4664-2022-2-4-13
24. Alkhimov Yu.V., Gnyusov S.F., Kapranov B.I., Klimenov V.A., Orishich A.M. Investigation of laser-welded titanium and stainless steel specimens using digital radiography methods. *Russian Journal of Nondestructive Testing*. 2012;48(4):238—244.
https://doi.org/10.1134/S106183091204002X

Information about the authors

Sergey V. Anakhov – Dr. Sci. (Eng.), Associate Professor, Head of the Department of mathematical and natural sciences, Russian State Vocational Pedagogical University (RSVPU).
https://orcid.org/0000-0003-1460-6305
E-mail: sergej.anahov@rsvpu.ru

Boris N. Guzanov – Dr. Sci. (Eng.), Professor, Head of the Department of engineering and vocational training in mechanical engineering and metallurgy, RSVPU.
https://orcid.org/0000-0001-5698-0018
E-mail: guzanov_bn@mail.ru

Nikolay S. Michurov – Senior Lecturer, Department of fire safety in construction, Ural Institute of State Fire Service of EMERCOM of Russia.
https://orcid.org/0000-0003-1775-6181
E-mail: n.michurov@ya.ru

Информация об авторах

Сергей Вадимович Анахов – д.т.н., доцент, заведующий кафедрой математических и естественно-научных дисциплин Российского государственного профессионально-педагогического университета (РГППУ).
https://orcid.org/0000-0003-1460-6305
E-mail: sergej.anahov@rsvpu.ru

Борис Николаевич Гузанов – д.т.н., проф., заведующий кафедрой инжиниринга и профессионального обучения в машиностроении и металлургии РГППУ.
https://orcid.org/0000-0001-5698-0018
E-mail: guzanov_bn@mail.ru

Николай Сергеевич Мичуров – ст. преподаватель кафедры пожарной безопасности в строительстве Уральского института ГПС МЧС России.
https://orcid.org/0000-0003-1775-6181
E-mail: n.michurov@ya.ru

Contribution of the authors

S.V. Anakhov – formulation of the research objective and tasks, preparation of the manuscript, and formulation of conclusions.

B.N. Guzanov – scientific supervision, development of the main concept, and revision of the manuscript and conclusions.

N.S. Michurov – preparation and execution of experiments, calculations, and manuscript preparation.

Вклад авторов

С.В. Анахов – постановка цели и задачи исследования, подготовка текста статьи, формулировка выводов.

Б.Н. Гузанов – научное руководство, формирование основной концепции, корректировка текста и выводов.

Н.С. Мичуров – подготовка и проведение экспериментов, осуществление расчетов, подготовка текста статьи.

The article was submitted 11.09.2024, revised 01.10.2024, accepted for publication 06.11.2024

Статья поступила в редакцию 11.09.2024, доработана 01.10.2024, подписана в печать 06.11.2024